sustainability

MDPI

Article

Optimal Allocation of Fast Charging Station for Integrated Electric-Transportation System Using Multi-Objective Approach

Ajit Kumar Mohanty [1], Perli Suresh Babu [1] and Surender Reddy Salkuti [2,*]

[1] Electrical Engineering Department, National Institute of Technology Warangal, Warangal 506004, India
[2] Department of Railroad and Electrical Engineering, Woosong University, Daejeon 34606, Korea
* Correspondence: surender@wsu.ac.kr

Abstract: The usage of Electric Vehicles (EVs) for transportation is expected to continue growing, which opens up new possibilities for creating new smart grids. It offers a large-scale penetration of Fast Charging Stations (FCE) in a local utility network. A severe voltage fluctuation and increased active power loss might result from the inappropriate placement of the FCE as it penetrates the Distribution System (DST). This paper proposes a multi-objective optimisation for the simultaneous optimal allocation of FCEs, Distributed Generators (DGs), and Shunted Capacitors (SCs). The proposed Pareto dominance-based hybrid methodology incorporates the advantages of the Grey Wolf Optimiser and Particle Swarm Optimisation algorithm to minimise the objectives on 118 bus radial distribution systems. The proposed method outperforms some other existing algorithms in terms of minimising (a) active power loss costs of the distribution system, (b) voltage deviations, (c) FCE development costs, (d) EV energy consumption costs, and (e) DG costs, as well as satisfying the number of FCEs and EVs in all zones based on transportation and the electrical network. The simulation results demonstrate that the simultaneous deployment technique yields better outcomes, such as the active power loss costs of the distribution system being reduced to 53.21%, voltage deviations being reduced to 68.99%, FCE development costs being reduced to 22.56%, EV energy consumption costs being reduced to 19.8%, and DG costs being reduced to 5.1%.

Keywords: electric vehicles; distribution system; distributed generators; shunted capacitor; fast charging station

Citation: Mohanty, A.K.; Suresh Babu, P.; Salkuti, S.R. Optimal Allocation of Fast Charging Station for Integrated Electric-Transportation System Using Multi-Objective Approach. *Sustainability* **2022**, *14*, 14731. https://doi.org/10.3390/su142214731

Academic Editors: Seyed Masoud Mohseni-Bonab, Ali Moeini and Ali Hajebrahimi

Received: 5 October 2022
Accepted: 4 November 2022
Published: 8 November 2022

1. Introduction

Climate change is one of the major concerns due to the enormous discharge of greenhouse gas because of the burning of fossil fuels. Carbon dioxide is one of the leading greenhouse gases responsible for a rising global temperature. Many countries are taking serious steps to curb the carbon footprint, such as renewable energy [1]. Renewable energy is essential to a power system's environment and energy economy. Replacing conventional combustion fuel with Electric Vehicles (EVs) is an economical and viable way to change [2,3]. Many nations have fixed the goal of 100% EV penetration in the future [4]. Due to this trend, the demand for FCEs and DGs in the DST is rising. The utility operators use SCs to improve the voltage profile in the distributed system. The improper allocation of FCE, DGs, and SCs negatively impacts the performance of DST. The proper distribution of FCEs and renewable energy sources could reduce barriers to EV adoption on a large scale and make sure that users of EVs can quickly obtain FCE [5].

Many researchers have stressed the impact and complexities of EVs on the distribution system [6–8]. Different models are developed [9–12] to reduce the uncertainties caused by EV mobility and to enhance environmental and economic benefits. By promoting this FCE infrastructure, with less worry about running out of power, EVs might travel more considerable distances. Existing studies consider power supply and transportation while preparing

for the rising penetration of FCE. The operating and capital costs should be considered when planning FCEs on the power supply side [13]. Additional complexities could be introduced by EV's rapid loading traits [14,15] and battery health [16,17]. Fahmy et al. [18] developed electric grid generic topologies where charging stations are connected to solve the challenges of EV aggregators. Yufei Wang et al. [19] suggested a setup strategy for flywheel energy storage systems for FCE. Regarding transportation, FCE's location must allow for an extensive and efficient travel service because it is a capital-intensive part of the transportation network [20]. Aside from that, the planning paradigm has also considered individual PEV drivers' mobility when using an acceptable spatial and temporal resolution [21]. L Bitencour et al. [22] developed a methodology where the semi-fast charging station is placed optimally in the neighbourhood. Dong et al. [23] developed a strategy for pricing FCEs to control voltage. Wang et al. [24] investigated the problem of FCEs in a highway with constraints such as budget and service capacities using a Bat Algorithm (BA).

Even while the power supply and transportation were addressed independently in previous works, FCE placement design necessitates the simultaneous consideration of these issues. Ignoring one or the other could result in poor economic choices, and even issues with the operation of the Transportation System (TN) or the electrical grid. For instance, placing an FCE near the feeder's head may be beneficial for reducing power delivery losses. However, due to geographical limitations, EV drivers might find it harder to reach this area. Xiang et al. [25] considered FCE's operational and investment costs, taking traffic restrictions into their planning models. In order to ensure that the entire road network's route is serviced by at least one FCE, the research by Miljanic et al. [26] sought to determine the least amount of strategically placed charging stations using an Integer Linear Programming Technique (ILP). For the best positioning and sizing of the FCE, Sadeghi et al. [27] introduced a Mixed-Integer Non-Linear (MINLP) optimisation approach. The proposed approach considers various factors, including the cost of station development, EV-specific energy, power grid loss, the placement of electric substations, and urban roadways.

The planning model used in the above articles has merely assigned the FCE, a frequent trait. At the same time, introducing EVs into the power grid may increase the energy loss, voltage drop, and peak load. In the literature, DGs are used as a planning tool to reduce the voltage drop and energy loss caused by the addition of the EV charging demand to the grid. Placing the FCE and DGs in the distribution system is covered by several research methods. Ajit et al. [28] proposed a model to place the FCE and DGs to reduce the distribution system's power loss and the cost of installing FCE. Battapothula et al. [29] suggested a model that minimises the network power loss and FCE installation cost as multi-objective optimisation problems to assign the FCE and DGs. Injeti et.al. [30] explained how optimally DGs could be integrated into EVs in the distribution system with an enhanced voltage profile system and decreased losses with a Butterfly Optimisation (BF) technique. Kumar et al. [31] developed a two-level framework. Regarding the first level of DST, DGs have been positioned optimally to reduce active power loss. The second level's optimal energy usage was carried out for the first level's location. Chang et al. [32] proposed a microgrid model that includes EVs. A renewable source powers charging stations. M. Ghofrani et al. [33] developed a framework where EVs and DGs are integrated into the DST based on operation and market aspects. Ahmad et al. [34] designed a framework for EMS for public EVs charging stations, integrating the microgrid depending on the market scenario. Rahmani-Andebili et al. [35] investigated the problems of DISCOs, i.e., the allocation of grid-based parking and management of an EV fleet.

In the literature cited above, DGs, which include solar panels, fuel cells, and micro-turbines, are described as an electrical source of energy that produces electricity at a unity power factor. SCs are utilised in distribution systems to meet reactive power requirements, where the power factor is improved. P Rajesh et al. [36] developed a methodology for the optimal allocation of the EV charging station in the presence of a capacitor, which enhances the DST's voltage profile and reduces power loss. Biswas et al. [37] discussed the

advantages of metaheuristic methods for determining the size and location of DGs and SCs in the DST to reduce the active power loss. Bilal et al. [38] presented that the optimal placement of the FCE and the capacitor reduces power loss and enhances the voltage profile of the DST.

Due to the relevance of FCE placement, significant literature on the subject has been published recently. Much of this research aims to minimise investment costs, transportation costs, energy loss, and voltage deviations, which can be accomplished using evolutionary algorithms such as Particle Swarm Optimisation (PSO) [39], Grey Wolf Optimisation (GWO) [40], JAYA algorithm [41] and Non-dominated sorting genetic algorithm-II (NSGA-2) [42]. Akanksha et al. [43] used the multi-objective GWO technique to identify non-dominated solutions and fuzzy satisfaction-based decisions to get at the final planning of FCE. Singh et al. [44] suggested a novel hybrid form that uses the advantages of both GWO and PSO. The primary goal of development is to increase the effectiveness for both types by strengthening the exploratory and exploitative capabilities of GWO and PSO.

Most authors cover the optimum placement of the FCE [6–27] or FCE and DGs [28–35] together. Few researchers consider the best placement of FCE, DGs, and SCs [36–38]. Voltage deviations (DVT), the development cost of the FCE (DFC), the cost of DGs (DGC), and the energy consumption of EV users are not discussed in those studies. In this study, the road network was integrated with a DST and placed optimally for FCE, DGs, and SCs simultaneously to minimise the active power loss costs of the distribution system (CPDN), DVT, FCE development costs (DFC), EUC, and DGC. Table 1 summarises the research gap analysis and the authors' contributions.

Table 1. An overview of the authors' work and the research gap analyses.

Ref.	DST	TN	FCE	DGs	SCs	Optimisation Strategies	DFC	EUC	CPDN	DVT	DGC
[20]	✓		✓			MILP		✓			
[21]	✓	✓	✓				✓	✓			
[24]	✓	✓	✓			BA			✓		
[26]		✓	✓			ILP	✓	✓			
[27]	✓	✓	✓			MILP	✓	✓	✓		
[28]	✓	✓	✓	✓		GWO	✓	✓	✓	✓	✓
[29]	✓	✓	✓	✓		NSGA-2	✓	✓	✓		✓
[30]	✓		✓	✓		BF	✓	✓		✓	
In this work	✓	✓	✓	✓	✓	GWO-PSO	✓	✓	✓	✓	✓

The following list outlines the paper's contribution step by step:

1. The optimal placement of the FCE and number of EVs considering active power loss, EV user behaviour, and DST voltage profile.
2. DGs' optimal sizing and location consider the FCE load to minimise real power loss and enhance DST's voltage profile.
3. Optimal placement of SCs considers the FCE load and DGs to improve the voltage profile of DST.
4. Simultaneous optimum placement of FCE, DGs, and SCs, considering EV user behaviour, real power loss, and DST voltage profile.

The remainder of this paper is structured as follows: Section 2 explains the formulation of the multi-objective issue and associated limitations. Section 3 presents the suggested hybrid GWO-PSO algorithm for the system under consideration. In Section 4, the results and analysis are covered. Section 5 discusses conclusions.

2. Problem Formulation

This section includes objective operations, such as DFC, EUC, CPDN, DVT and DGC being minimised.

In order to determine the optimal allocation of FCE, the proposed approach uses an arbitrary area, as depicted in Figure 1. Zones [45,46] are created inside the research

area, such as zn_1, zn_2, zn_3, and zn_4, where the number of EVs is available in each zone [29]. The assumption is that the number of EVs in each zone is located in the geographical centre. On a particular day, it was assumed that the FCE charges the Total Number of EVs ($NTEV$) in the considered area. $NTEV$ is calculated as:

$$NTEV = \sum_{z=1}^{zn} EV_{n,zn} \quad (1)$$

The number of committed EVs in the zone (zn) is represented by the value $EV_{n,zn}$.

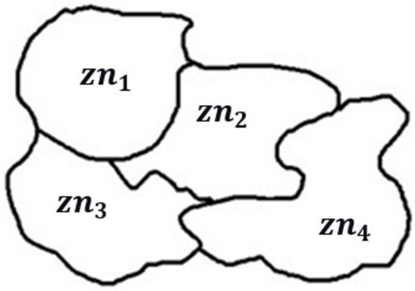

Figure 1. Illustrative zones with area.

2.1. Development Cost of FCEs (DFC)

DFC includes the cost of the charging station equipment and land cost. The equipment and land cost of charging station is a function of the number of charging connectors and capacity of charging stations [27].

$$DFC = C_{fixed} + 24 \times C_{land} \times NC(i) \times n_y + C_{cond} \times (NC(i) - 1) \times P_{cg} \quad (2)$$

FCE's fixed cost is denoted by C_{fixed} (USD). Since it deals with the equipment, the cost is almost similar among the different countries. C_{land} (in USD per meter) is the land rental cost yearly. The study time for the FCE consists of n_y years. The charger development cost is C_{cond}, $NC(i)$ is the number of connectors in charging stations in the ith FCE, and P_{cg} is the charging connector rated power (kW).

$$NC(i) = \sum_{z=1}^{zn} (max(PR_{EV}) \times EV_{n,zn} \times DFE(z,i)) \quad (3)$$

The probability that EVs will be charged in an hour (h) during a day is PR_{EV}. $DFE(z,i)$ is a decision binary variable, and if EVs in the zn are charged in the ith FCE, then $DFE(z,i) = 1$; otherwise, it is zero. The choice of EVs in the zn to the ith FCE is calculated by the minimal distance between the ith FCE to zn compared to the other FCE.

The capacity of the charging station's connectors differs between 50–250 kW. The rating of the ith FCE is calculated as:

$$P_{FCE} = NC(i) \times P_{cg} \quad (4)$$

2.2. Energy Consumption of EVs User Cost (EUC)

The EV user takes a particular route to reach the FCE. While driving, the EV consumes energy, and the cost related to energy consumption is represented by the EUC. In order to charge the batteries of EVs, which are situated at location zone zn to the nearest ith FCE, $EUC(zn,i)$ is calculated as [27]:

$$EUC(zn,i) = L(zn,i) \times CSE \times \sum_{hr=1}^{24} PR_{EV}(h) \times EV(zn) \times EP_h \quad (5)$$

The distance between the ith FCE and zone (zn) on a trajectory length is denoted as $L(zn,i)$. The electricity price in USD is represented by EP_h, and CSE is the specific energy consumption of EVs. EVs' CSE stands for their specific energy consumption.

2.3. Active Power Loss of Distribution Network Cost (CPDN)

Since the EV demand is increasing, the load in the distribution network increases and distribution network power losses also increase. A non-linear relationship exists between the loading and the distribution network loss. The load varies from hour to hour on a particular day and during the year. A correct estimation of the distribution network power loss due to EV charging is required, i.e., the load variation must be considered. The Active power loss of the Distribution Network Cost ($CPDN$) [27] of all seasons in a year is calculated as:

$$CPDN = \sum_{s=1}^{n_s} \sum_{hr=1}^{24} TPL(hr, s) \times N_{hr}(s) \times EP_h \tag{6}$$

The number of seasons is denoted as n_s, and TPL is the active power loss of the DST, including EV loads. The total number of hours throughout all seasons in a year is N_{hr}.

2.4. Cost of DGs (DGC)

The cost of DGs includes the cost of investment C_{INV}, the cost of operation C_{OPR}, and the cost of maintenance C_{MAT} of DGs [29].

1. Cost of Investment: this includes various initial costs, such as money invested on unit construction, essential equipment, and installation for each generation unit. This cost can be expressed as:

$$C_{INV} = \sum_{d=1}^{ndg} (P_{dg,d} \times Cost_{INV}) \tag{7}$$

2. Cost of operation: the generation cost, fuel cost, and other similar costs are considered in the cost of operation C_{OPR}. It can be formulated as

$$C_{OPR} = \sum_{yr=1}^{n_{yr}} \sum_{d=1}^{n_{dg}} \left(P_{dg,d} \times TL_h \times CO_d \times \left(\frac{1 + R_I NF}{1 + R_I NT} \right)^{yr} \right) \tag{8}$$

3. Cost of Maintenance: This includes the cost required for restoring the unit equipment, renewal, and repairing.

$$C_{MAT} = \sum_{yr=1}^{n_{yr}} \sum_{d=1}^{n_{dg}} \left(P_{dg,d} \times TL_h \times CM_d \times \left(\frac{1 + R_I NF}{1 + R_I NT} \right)^{yr} \right) \tag{9}$$

Hours in a year are denoted by TL_h. The number of DGs considered for this study is n_{dg}, with n_{yr} being the total years for DG planning. Lastly, the DGC can be determined as:

$$DGC = C_{INV} + C_{OPR} + C_{MAT} \tag{10}$$

2.5. DVT

The improper placement of the FCE and DGs in the DST leads to voltage instability. This work calculates voltage deviations for 24 h of all seasons. Calculating the DVT of DST is as follows:

$$DVT = max\{1 - V(j)\} \qquad j = 1, 2 \ldots nb \tag{11}$$

The voltage of the jth bus is $V(j)$, and the DST bus number is nb.

2.6. Objective Problems

The optimum number of FCEs obtained using the proposed optimisation procedure is denoted by the symbol N_{FCE}. The primary purpose of the objective problem is to minimise the DFC, EUC, $CPDN$, DVT, and DGC by satisfying the constraints.

$$Min \left\{ \sum_{k=1}^{N_{FCE}} DFC(k) + \sum_{l=1}^{NTEV} EUC(l) + CPDN + DGC + DVT \right\} \tag{12}$$

Constraints

To recharge the EVs from the research area, one FCE must be installed.

$$\sum_{k=1}^{NP_{FCE}} B(k) > 0 \qquad k = 1, 2, 3 \ldots, \ NP_{FCE} \tag{13}$$

$B(k)$ is a binary decision variable; if the kth FCE is chosen, $B(k) = 1$; otherwise, $B(k) = 0$. NP_{FCE} is the number of feasible FCEs. At least one connector should be taken into account from the chosen FCE.

$$NC(k) \geq 0 \qquad k = 1, 2, 3 \ldots, \ NP_{FCE} \tag{14}$$

One optimal FCE is chosen by EVs from each zn depending on the displacement between zn to the kth FCE.

$$\sum_{z=1}^{zn} DFC(z, k) \times B(k) = 1 \tag{15}$$

3. Overview of Hybrid GWO-PSO Algorithm

In the real world, the power system has multiple objective functions that should be optimised simultaneously. The objective function suggested in this work is optimised using a hybrid GWO-PSO technique [44]. The best features of GWO and PSO are combined to solve the problems. PSO [39] is a population-based metaheuristic optimisation algorithm. The greatest advantages of PSO is that it is simple to perform and has fewer controlling parameters.

$$Z_{p+1}^{itr} = \ Z_p^{itr} + v_{p+1}^{itr} \tag{16}$$

$$v_{p+1}^{itr} = v_p^{itr} + c_1 \times ran1 \times \left(P_{best}^{itr} - Z_p^{itr}\right) + c_2 \times ran2 \times \left(G_{best}^{itr} - Z_p^{itr}\right) \tag{17}$$

Here, Z_p is the position vector, v_p is the velocity vector, itr is the iteration, p is the particle in the population, w is the inertia of the weight parameter, P_{best}^{itr} is the best position in the pth particle and G_{best}^{itr} is the best position in the available population. In the PSO algorithm, the main disadvantage is that the updated position and velocity of a particle cannot jump into another space with a global optimum and has a low convergence rate in the iterative process.

Grey Wolf Optimisation (GWO) [40] is an intelligent swarm technique. GWO follows the hierarchy of leadership. Grey wolves are well coordinated and always live in packs. They always follow the social hierarchy, and, based on this hierarchy, they can be classified into four types of wolves, i.e., Alpha (α), Beta (β), Delta (δ), and Omega (ω). This social hierarchy is based on their fitness value. α is the top leader and makes the decisions (hunting, staying in one place, sleeping, etc.), and other members follow the order. β is subordinate to α, where β helps give suggestions to α for decision making and always ensures that other members follow the order given by α. δ is subordinate to β but superior to ω. ω is the follower and occupies the minuscule level in the hierarchy.

3.1. Encircling the Victim

During hunting, they encircle the prey. Encircling mathematical behaviour is modelled as

$$\vec{L} = \left|\vec{S}.\vec{Z}_p - \vec{Z}(itr)\right| \tag{18}$$

$$\vec{Z}(itr) = \vec{Z}_p(itr) - \vec{R}.\vec{L}t \tag{19}$$

itr denotes the current iteration, Z_p depicts the location of the prey, and Z represents the positioning of the grey wolf. It is possible to determine the vector coefficients $\vec{S}$ and $\vec{R}$ as

$$\vec{R} = 2.\vec{r}.rad_1 - \vec{r} \tag{20}$$

$$\vec{S} = 2.rad_2 \tag{21}$$

[0, 1] are the boundaries of the random vectors rad_1, rad_2. Through iterations, the coefficient $\vec{r}$ linearly declines from 2 to 0.

3.2. Hunting Procedure

α provides direction for the hunting process. A deeper understanding of the prey (optimal solution) is held by α, β, and δ. As alpha, beta, and delta change positions, other wolves in the back update the positions. Attacking can be expressed mathematically as follows:

$$\vec{L_\alpha} = \left|\vec{S}.\vec{Z_\alpha} - \vec{Z}\right| \tag{22}$$

$$\vec{L_\beta} = \left|\vec{S}.\vec{Z_\beta} - \vec{Z}\right| \tag{23}$$

$$\vec{L_\delta} = \left|\vec{S}.\vec{Z_\delta} - \vec{Z}\right| \tag{24}$$

$$\vec{Z_1} = \vec{Z_\alpha} - \vec{R_1}.(\vec{L_\alpha}) \tag{25}$$

$$\vec{Z_2} = \vec{Z_\beta} - \vec{R_2}.(\vec{L_\beta}) \tag{26}$$

$$\vec{Z_3} = \vec{Z_\delta} - \vec{R_3}.(\vec{L_\delta}) \tag{27}$$

$$\vec{Z}(itr+1) = \frac{\vec{Z_1} + \vec{Z_2} + \vec{Z_3}}{3} \tag{28}$$

3.3. Exploring and Attacking a Victim

When wolves attack their prey, and $|R| < 1$, the R-value should fall between [−2r, 2r]. Exploitation is the act of attacking prey. Exploration is the process through which they separate to look for the target. If $|R| > 1$, wolves are compelled to look for prey.

3.4. Hybrid GWO-PSO

Singh et al. [44] used low-level co-evolution mix hybrids for hybridising GWO with the PSO method. This algorithm's design philosophy integrates the GWO algorithm's exploration capability with the PSO algorithm's exploitation capability to maximise both types' strengths. The exploration and exploitation of the grey wolves in the search area are controlled by the inertia constant (w) rather than conventional mathematical calculations. The suggested equations update the positions of the first three agents in the search space.

$$\vec{L_\alpha} = \left|\vec{S}.\vec{Z_\alpha} - w \times \vec{Z}\right| \tag{29}$$

$$\vec{L_\beta} = \left|\vec{S}.\vec{Z_\beta} - w \times \vec{Z}\right| \tag{30}$$

$$\vec{L_\delta} = \left|\vec{S}.\vec{Z_\delta} - w \times \vec{Z}\right| \tag{31}$$

By revising the velocity and locations' equations as below, the GWO and PSO variants are combined.

$$s = (v_p^{itr} + c_1 \times ran1 \times \left(\vec{Z_1} - Z_p^{itr}\right) + c_2 \times ran2 \times \left(\vec{Z_2} - Z_p^{itr}\right) + c_3 \times ran2 \times \left(\vec{Z_3} - Z_p^{itr}\right) \tag{32}$$

$$v_{p+1}^{itr} = w \times \left(v_p^{itr} + s\right) \tag{33}$$

$$Z_{p+1}^{itr} = Z_p^{itr} + v_{p+1}^{itr} \tag{34}$$

Figure 2 depicts the hybrid GWO-PSO algorithm's flowchart. The hybrid GWO-PSO process' basic steps are as follows:

1. Initialise the parameters of GWO and PSO $\vec{R}$, $\vec{S}$, $\vec{r}$ and w; // w = 0.5 + rand()/2 and set maximum iteration.
2. Calculate an agent's fitness using Equations (29)–(31).
3. Update the velocity and location of the current search's grey wolf for each search using Equations (33) and (34).
4. $\vec{R}$, $\vec{S}$, and $\vec{r}$, are updated, Fitness of all wolves are computed.
5. Positions of α, β, and δ are updated
6. Until the terminating requirements are met, repeat this process.

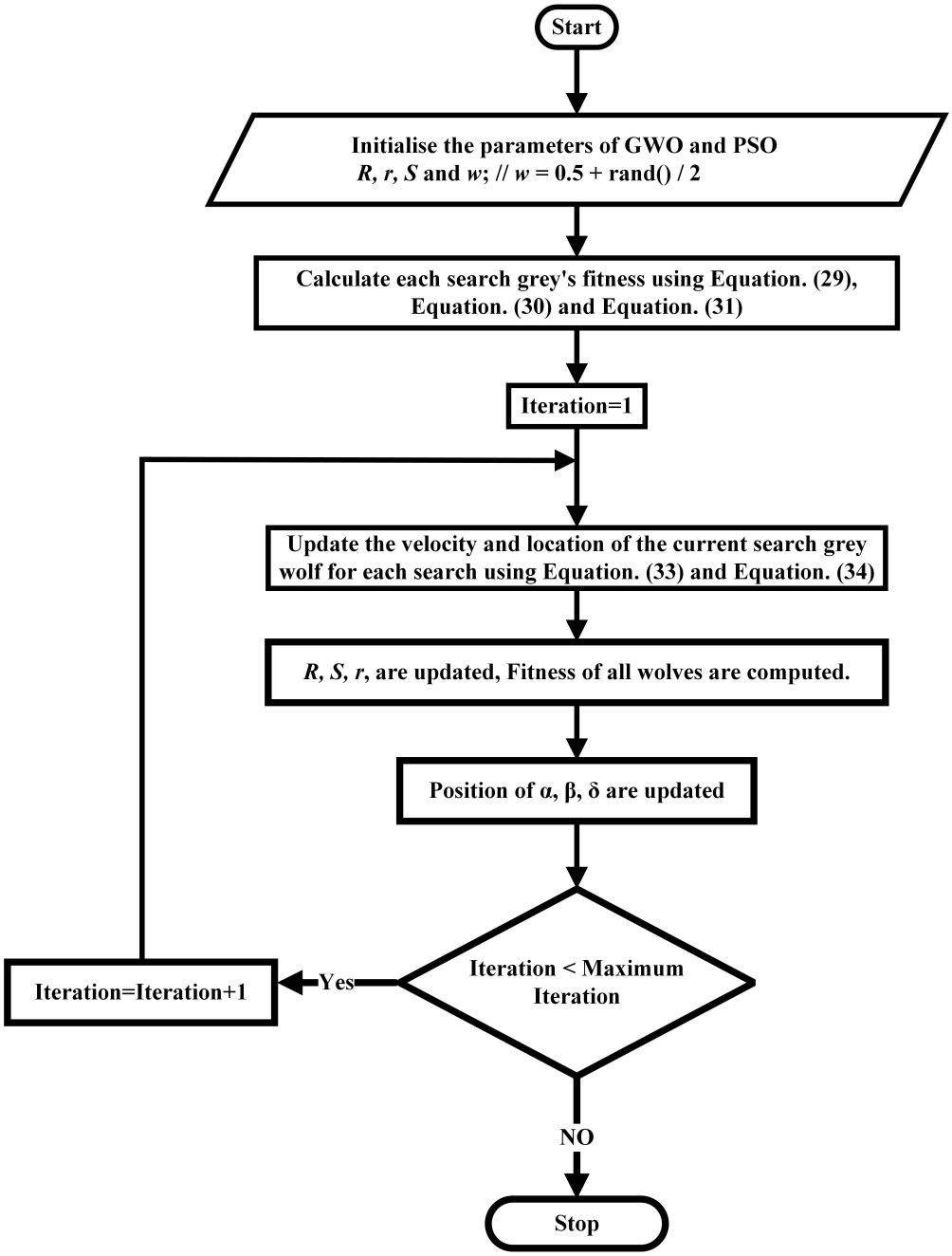

Figure 2. Hybrid GWO-PSO flowchart.

The multiple objective functions are constructed as a single goal function by selecting appropriate weights for each objective in all traditional approaches, such as the weighted objective approach. There are primarily two issues with determining the single objective's optimal value. The first is that while optimising a single objective function might ensure

the existence of a single optimal solution, in all practical uses, the judgement still wants access to other solutions. The second examines how each goal in a single objection function responds to its weights. Additionally, the classical approaches are ineffective when the objective function is much noisier, and the factors in the search area are discontinuous.

Multi-objective Pareto front optimisation techniques are required to address multi-objective scenarios to get around the abovementioned issues. The hybrid methods are also quite effective at locating the best solution. In this work, hybrid GWO-PSO was utilised to meet the desired objectives. Mirjalili et al. [47] proposed a set of non-dominated solutions, and one of these solutions must be chosen by the decision maker. Due to the subjectively inaccurate nature of the decision maker's assessment and the fact that it is straightforward to employ and has similarities to human thinking, the fuzzy satisfaction-based method [43] was employed in this case for ultimate decision-making.

4. Results and Discussion

In this study, four scenarios with various cases were explored using the suggested test system to determine the optimum distribution of FCE, DGs, and SCs in a connected transportation network.

4.1. Proposed Methodology

This study used a 720 km^2 test area to apply the suggested strategy [29]. The population of EVs in each research area zone is shown in Figure 3. There are 180 zones in the test area, each with a 4 km^2 (2 km × 2 km). As seen in Figure 4, a test area was connected to the 118 bus radial distribution system [29].

0	3	5	3	4	6	4	0	0	3	7	5	6	4	0
3	5	4	6	4	6	7	8	7	9	8	7	5	6	4
7	11	16	9	9	13	12	10	11	14	17	6	9	5	3
6	1	7	15	16	17	17	9	15	7	14	17	9	15	1
4	6	9	10	8	16	16	14	0	14	16	11	7	9	7
0	13	14	10	16	14	19	15	17	14	12	8	15	9	4
7	11	0	16	16	17	13	18	17	15	9	19	12	8	0
4	9	15	14	12	11	4	16	19	9	12	17	17	12	6
8	13	14	19	17	15	17	0	13	12	11	13	9	15	8
3	12	9	16	13	14	9	14	16	15	17	16	15	13	3
0	6	7	8	7	5	6	4	8	5	4	6	4	0	0
0	5	3	4	6	4	0	7	3	0	5	6	4	3	4

Figure 3. Zone EV population.

In this paper, the total EV population was considered as 1632. With the requirement that each FCE is roughly equally spaced apart, it has been assumed that 16 FCE might be put along the test area's major roadways. Figure 4 depicts 16 possible FCEs represented in the DST by the rhombus symbol. The simulation of the proposed problem was carried out in MATLAB 2017a software installed on a computer with a processor intel core i5 8th Gen and 8 GB RAM. A 118 distribution bus system was considered to carry out the analysis. The distributed system's base values were as follows: 22.71 MW of real power, 11 kV, 100 MW, and 1.7041 MVAr [29]. The load curve [27] for different seasons is shown in Figure 5. For the optimum location and sizing of DGs and SCs in the distribution system, this paper considered five bus nodes of DGs units and three bus nodes of SCs units. From 5 a.m. to 9 p.m. every day, it is presumable that EVs are charged at the FCE. Figure 6 indicates the probability of daily EV charging. The DST and FCE parameters are represented in Table 2. Four different scenarios were analysed with the help of a hybrid GWO-PSO algorithm with a maximum of 500 iterations for appraising the proposed problem.

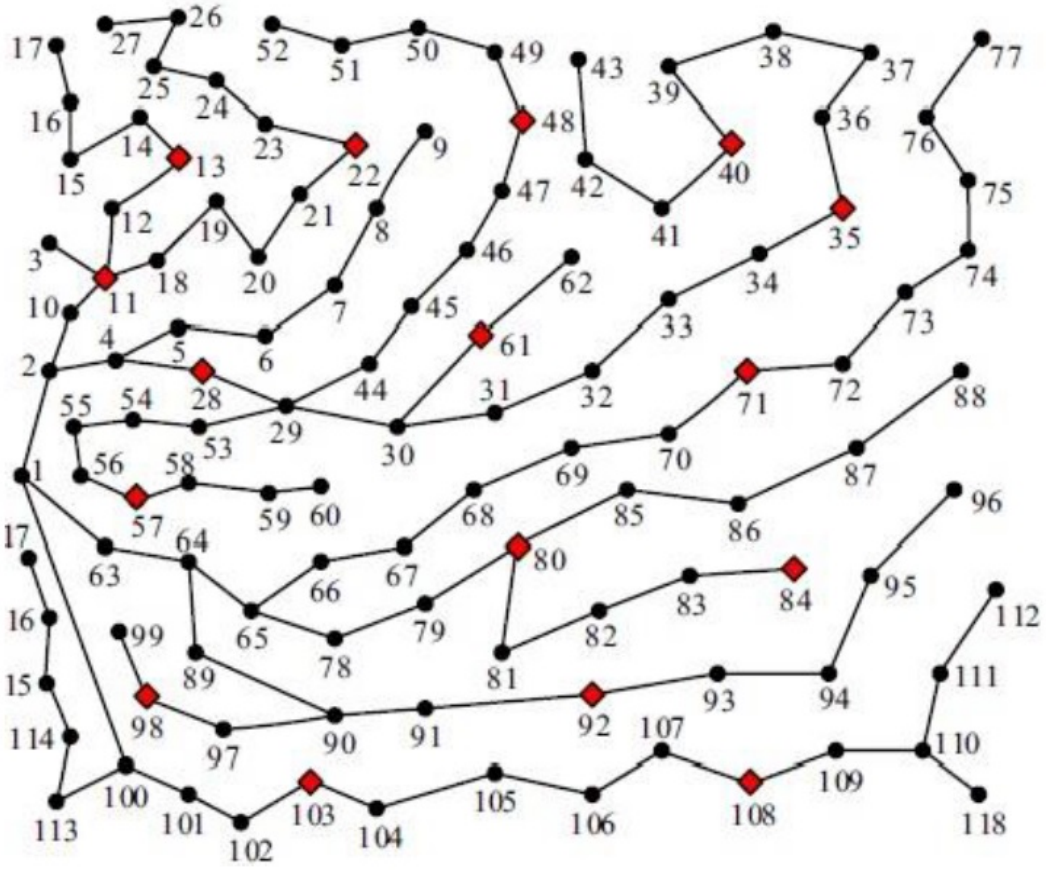

Figure 4. 118 bus distribution system in the proposed testing area.

Table 2. Study parameters.

Parameter	Values
NTEV	1632
n_y	5
NP_{FCE}	16
CSE	0.142 kWh/km
EP_h	USD 87.7/MWh
C_{land}	USD 240/M2 per year
C_{fixed}	USD 70,000
C_{cond}	USD 208.33/kW
P_{cg}	96 kW

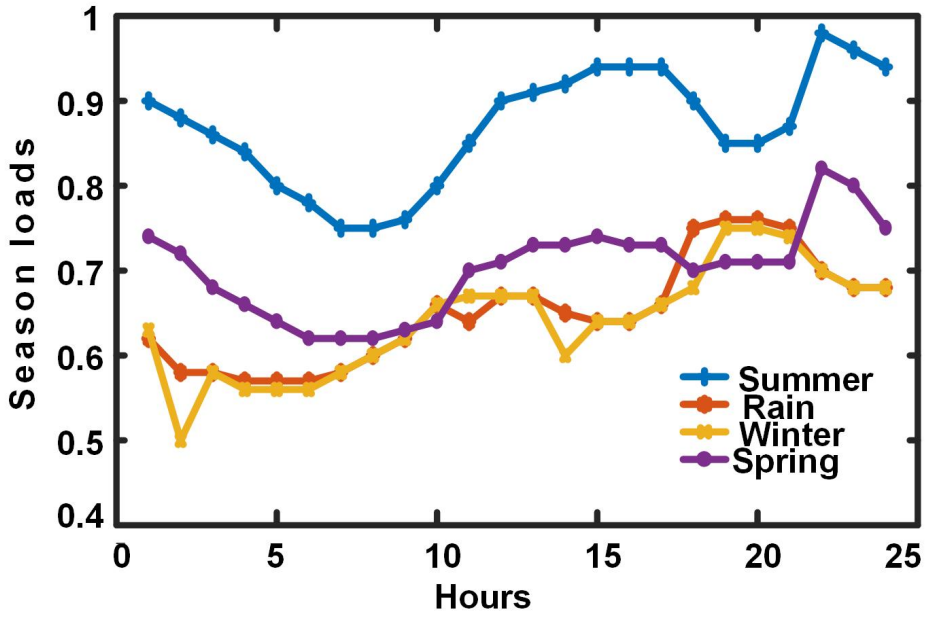

Figure 5. Load curve on an hourly basis for various seasons.

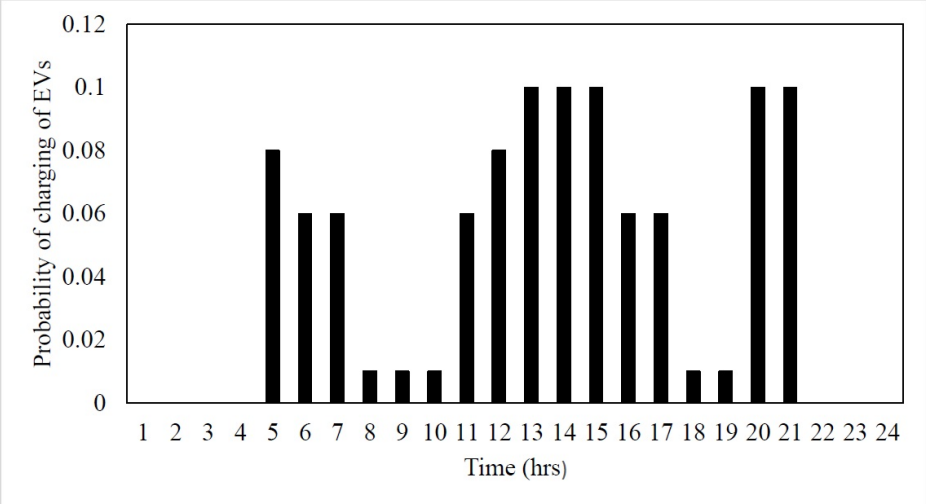

Figure 6. EVs' probability of being charged.

Due to its simple and independent structure from the problem, an optimisation method utilised in planning FCE, DGs, and SCs can be applied to any test system. Additionally, the fuzzy satisfaction-based choice approach [43] allows decision makers to select the ultimate organising strategy under their preferences by selecting preferred values.

4.2. Scenario 1: Optimum Placement of FCE in DST Conjunction with Transportation Network

The optimal allocation of an FCE is achieved by minimising the EUC, CPDN, and DVT of the DST. DGs are not considered; therefore, DGC in Equation (12) is zero. Since the total number of connectors in FCEs is almost constant, the DFC variation has an almost negligible effect on the objective function. Thus, the DFC is not considered to minimise the objective function in this scenario. In this scenario, three cases are taken:

(a) Case 1: Minimisation of EUC and CPDN.
(b) Case 2: Minimisation of DVT and CPDN.
(c) Case 3: Minimisation of DVT, CPDN, and EUC.

The optimal Pareto font for various cases in scenario 1 shows figures from Figure 7a–c. The best location and size of the FCE are obtained from the fuzzy satisfaction-based choice approach [43]. Table 3 displays the optimum FCE position and EV values, whereas Table 4 displays the optimal objective parameters.

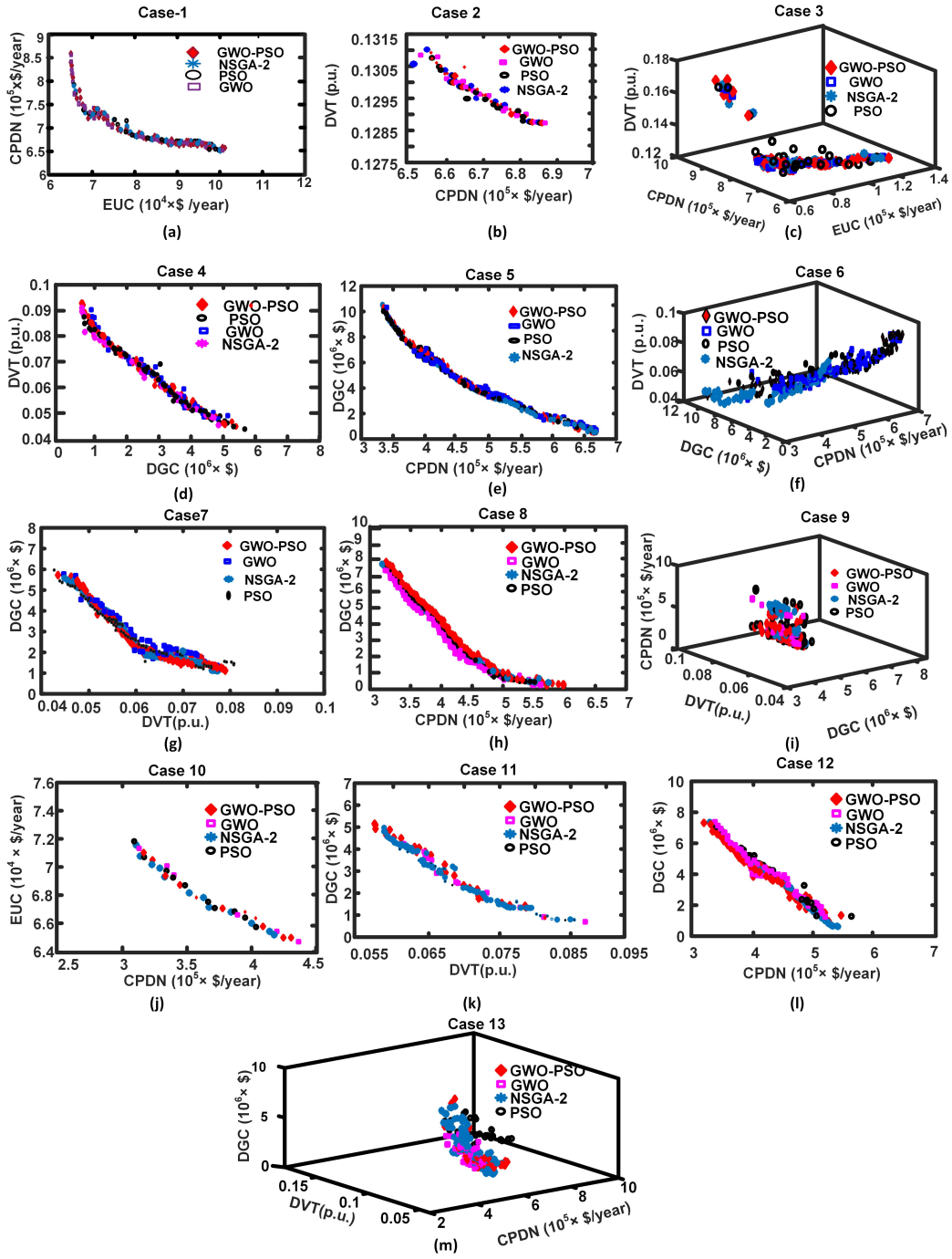

Figure 7. Optimal Pareto-front.

Table 3. The optimum FCE location and the optimum number of EVs.

Cases	NSGA -2		PSO		GWO		GWO-PSO	
	FCE Location	Number of EVs	FCE Location	Number of EVs	FCE Location	Number of EVs	FCE Location	Number of EVs
Case-1	80	559	22	291	40	291	22	239
	103	83	35	413	11	170	11	170
	40	395	13	122	80	413	80	413
	13	112	80	397	13	137	13	122
	22	329	11	170	22	224	40	291
	11	154	40	239	35	397	35	397
Case-2	11	370	11	114	40	344	11	408
	22	253	28	170	61	173	28	114
	35	408	40	253	22	177	84	253
	28	114	22	285	11	150	35	370
	40	210	80	397	35	383	22	277
	84	277	35	413	80	405	28	114
Case-3	40	383	13	137	11	170	13	137
	61	177	11	170	28	114	11	170
	22	173	22	291	40	285	22	224
	11	150	80	397	22	253	80	413
	35	344	40	224	80	413	40	291
	80	405	35	413	35	397	35	397

Table 4. Objectives of scenario 1 that are optimal.

Algorithms	Cases	DFC (USD M)	EUC (USD M/year)	CPDN (USD M/year)	DVT (p.u.)
NSGA -2	1	4.2235	0.09233	0.6823	0.1325
	2	4.2225	0.09422	0.67730	0.1309
	3	4.2614	0.09078	0.68153	0.1308
PSO	1	4.2312	0.103231	0.69853	0.1345
	2	4.2309	0.105019	0.68730	0.1319
	3	4.3301	0.103618	0.69853	0.13173
GWO	1	4.2152	0.085878	0.68243	0.1308
	2	4.2140	0.086632	0.66840	0.1301
	3	4.224	0.084653	0.68129	0.1300
GWO-PSO	1	4.2053	0.084778	0. 67464	0.1301
	2	4.2052	0.08532	0.66730	0.1300
	3	4.15	0.083618	0.67129	0.1295

4.3. Scenario 2: Optimal Positioning of DGs in DST with Previous Optimum FCE Load

DGs enhance the voltage profile and lower power losses in the DST. For the optimal DGs positioning, the optimal FCE load from case 3 is taken into account. This scenario takes into account three cases.

(a) Case 4: Minimisation of DGC and DVT.
(b) Case 5: Minimisation of CPDN and DGC.

(c) Case 6: Minimisation of DGC, DVT, and CPDN.

Figure 7d–f are displayed using the best pareto-front for various scenarios in scenario 2. The optimal location and size of DGs are obtained from the fuzzy satisfaction-based choice approach. For various cases in scenario 2, the optimum location and sizing of DGs are displayed in Table 5, and objective parameters are depicted in Table 6.

Table 5. Scenario 2: Optimal location and sizing of DGs.

Cases	NSGA -2		PSO		GWO		GWO-PSO	
	DGs Location	DGs Size (MW)	DGs Location	DGs Size (MW)	DGs Location	DGsSize (MW)	DGs Location	DGs Size (MW)
Case-4	102	0.5020	75	0.5118	43	0.3764	49	0.2138
	75	0.7563	73	0.7723	77	0.9332	54	1.1365
	42	0.5002	48	0.9579	50	0.2400	72	0.1730
	62	0.5039	52	0.6249	53	0.7050	111	0.5406
	51	0.6407	108	0.5352	110	0.3217	76	0.9215
Case-5	73	1.3467	49	0.5641	47	0.7505	51	0.2895
	35	1.3012	113	0.8880	72	0.7327	84	0.9365
	80	1.1789	51	0.8688	75	0.5569	111	0.6758
	111	1.0722	83	0.6051	111	1.2189	74	1.0127
	51	0.6969	73	1.1742	50	0.8504	48	0.5020
Case-6	111	1.0385	110	1.2682	76	0.9847	54	1.5878
	74	1.4989	74	1.4116	111	0.8272	73	1.4037
	42	0.7511	82	0.5486	53	0.7631	83	1.0371
	54	0.9941	50	1.1380	70	0.7140	111	0.7847
	49	0.8780	53	0.7769	49	0.8662	96	1.1010

Table 6. Objectives of scenario 2 that are optimal.

Algorithms	Cases	CPDN (USD M/year)	DGC (USD M)	DVT (p.u.)
NSGA -2	4	0.5278	3.5326	0.0677
	5	0.4398	6.8091	0.0565
	6	0.4081	6.2795	0.0462
PSO	4	0.476	4.1396	0.0592
	5	0.4404	4.9892	0.0566
	6	0.4042	7.1965	0.0457
GWO	4	0.5132	3.1348	0.0615
	5	0.4417	5.0003	0.0579
	6	0.4454	6.2583	0.0508
GWO-PSO	4	0.4931	3.6326	0.0564
	5	0.4750	4.1572	0.0684
	6	0.4051	5.0561	0.0503

4.4. Scenario 3: Allocation of DGs and SCs in DST Optimally Using the Previous Optimal FCE Load

The optimal positioning of DGs and SCs is considered in the distributed system to enhance the voltage profile of the system. Three cases are used in this scenario for the optimal planning of DGs and SCs with the optimum load of the FCE from case 3.

(a) Case 7: Minimisation of DGC and DVT.
(b) Case 8: Minimisation of CPDN and DGC.
(c) Case 9: Minimisation of DGC, DVT, and CPDN.

The optimal pareto font for various cases in scenario 3 shows figures from Figure 7g–i. The optimal location and size of DGs and SCs are obtained from the fuzzy satisfaction-based choice approach. For various cases in scenario 3, the optimal sizing and location of DGs are shown in Table 7, Table 8 shows the optimal SCs position and sizing, and Table 9 shows the objective parameters.

Table 7. DGs' optimal location and sizing for scenario 3.

Cases	NSGA -2		PSO		GWO		GWO-PSO	
	DGs Location	DGs Size (MW)	DGs Location	DGs Size (MW)	DGs Location	DGs Size (MW)	DGs Location	DGs Size (MW)
Case-7	75	0.4000	75	0.7629	17	0.1839	110	0.5540
	76	0.6827	71	0.1132	77	1.0291	47	0.3261
	26	0.1000	110	0.7330	103	0.1000	75	0.4110
	35	0.3800	72	1.3930	74	0.1000	77	0.4041
	54	0.2562	107	0.1000	46	0.1000	56	0.1276
Case-8	112	0.2264	72	0.8602	52	0.5007	75	0.5492
	51	0.3825	52	0.1674	86	0.4312	112	0.678
	110	0.4266	58	0.2686	52	0.2131	58	0.5035
	74	0.3401	25	0.1904	51	0.3846	62	0.5402
	15	0.1000	52	0.4417	71	0.3146	52	0.4235
Case-9	75	1.1995	118	0.6484	70	0.6849	73	0.2326
	47	1.6504	51	1.3910	110	0.8048	32	0.6461
	111	1.2904	70	1.6759	50	1.0038	77	1.6407
	8	0.3571	113	1.1950	75	0.8921	53	2.0730
	60	0.3935	76	0.5228	84	0.6258	108	1.0549

Table 8. Optimal location and sizing of SCs for scenario 3.

Cases	NSGA -2		PSO		GWO		GWO-PSO	
	Location of SCs	Size of SCs (MVAr)	Location of SCs	Size of SCs (MVAr)	Location of SCs	Size of SCs (MVAr)	Location of SCs	Size of SCs (MVAr)
Case-7	48	0.6744	53	0.9704	38	0.1000	51	0.9504
	111	0.7627	61	0.1462	37	1.0000	35	0.3564
	21	0.7187	51	0.7401	48	0.3198	71	0.5740
Case-8	50	1.0000	51	0.5544	54	0.7152	111	0.9558
	70	1.0000	73	1.0000	11	0.8494	71	0.7703
	20	0.4638	109	0.9516	75	0.8960	35	0.7908
Case-9	50	0.6739	52	0.9023	51	0.9796	112	1.0000
	53	0.4210	57	0.8283	72	0.5760	75	0.8276
	77	0.4206	37	1.0000	95	0.8905	52	0.8558

Table 9. Scenario 3's optimal objective parameters.

Algorithms	Cases	CPDN (USD M/year)	DGC (USD M)	DVT (p.u.)
NSGA -2	7	0.49264	2.2132	0.0602
	8	0.5027	1.7956	0.0674
	9	0.37133	5.9512	0.0447
PSO	7	0.4853	3.7746	0.0503
	8	0.4555	2.3463	0.0600
	9	0.3974	6.8717	0.044275
GWO	7	0.55122	2.2180	0.0688
	8	0.4714	3.2785	0.0679
	9	0.3811	5.0512	0.05014
GWO-PSO	7	0.48759	1.8410	0.0560
	8	0.4295	2.2440	0.0621
	9	0.3402	4.8811	0.04287

4.5. Scenario 4: Simultaneous Optimum Location and Sizing of FCE, DGs, and SCs in DST

In this scenario, the optimum location and sizing of the FCE, DGs, and SC in a DST is achieved by coupling a transportation network to reduce the cost of CPDN, EUC, DGC, and DVT. The following four cases are considered.

(a) Case 10: Minimisation of CPDN and EUC.
(b) Case 11: Minimisation of DGC and DVT.
(c) Case 12: Minimisation of CPDN and DGC.
(d) Case 13: Minimisation of DGC, DVT, and CPDN.

The optimal Pareto font for various cases is scenario 4, which shows figures from Figure 7j–m. The best location and size of FCE, DGs, and SCs are obtained from the fuzzy satisfaction-based choice approach. For various cases in scenario 4, the optimal allocation of the FCE, number of EVs, DGs, and SCs is shown in Tables 10–12. The objective is the parameters that are shown in Table 13.

Table 10. Optimal FCE location and EVs optimal numbers in scenario 4.

Cases	NSGA -2		PSO		GWO		GWO-PSO	
	FCE Location	Numbers of EVs	FCE Location	Numbers of EVs	FCE Location	Numbers of EVs	FCE Location	Numbers of EVs
Case-10	28	159	103	192	103	192	57	268
	71	387	80	383	57	268	28	159
	80	364	71	368	80	310	80	310
	92	211	92	207	92	281	92	285
	98	220	98	220	71	319	71	319
	108	291	108	262	108	262	108	291
Case-11	22	199	57	187	40	301	22	222
	61	364	80	375	57	354	13	122
	103	123	84	419	22	183	40	216
	57	187	61	170	28	98	57	247
	80	395	40	308	61	309	84	439
	40	364	22	173	35	387	80	386

Table 10. *Cont.*

Cases	NSGA -2		PSO		GWO		GWO-PSO	
	FCE Location	Numbers of EVs	FCE Location	Numbers of EVs	FCE Location	Numbers of EVs	FCE Location	Numbers of EVs
Case-12	22	366	103	242	40	467	40	486
	98	60	80	371	22	332	11	193
	28	114	35	553	11	104	48	195
	57	641	57	233	57	143	28	72
	103	25	48	49	80	488	80	444
	40	426	13	184	28	98	13	242
Case-13	13	147	103	192	13	242	80	445
	71	437	80	383	28	72	48	86
	92	229	71	368	11	193	98	105
	80	320	92	207	40	486	92	678
	40	280	98	220	80	539	57	131
	57	219	108	262	48	100	28	187

Table 11. Optimal positioning and sizing of DGs for scenario 4.

Cases	NSGA -2		PSO		GWO		GWO-PSO	
	DGs Location	DGs Size (MW)	DGs Location	DGs Size (MW)	DGs Location	DGs Size (MW)	DGs Location	DGs Size (MW)
Case-10	51	1.6040	77	0.6379	91	1.9655	108	1.3820
	111	2.2000	71	1.8732	73	1.8865	102	1.0985
	71	2.2000	22	1.2961	64	2.1657	80	2.2000
	98	2.2000	65	1.9889	113	1.8273	50	1.9288
	75	0.9668	9	1.1762	109	1.0029	74	1.2749
Case-11	101	0.1000	25	0.9424	70	0.2873	70	0.3393
	113	0.4778	7	0.1220	34	0.2730	35	0.1000
	33	1.0544	75	0.1566	30	0.4431	118	0.1000
	59	0.1294	15	1.0951	81	0.1339	11	0.3617
	42	0.1696	74	0.5410	49	0.5244	61	0.5362
Case-12	39	0.1018	23	0.1000	87	0.2801	61	0.3517
	21	0.1000	32	0.1832	45	0.6059	77	0.9536
	23	0.3469	22	0.3884	56	0.2757	18	0.1517
	40	0.1653	21	0.5953	18	0.2410	4	0.1000
	35	0.1000	112	0.8418	71	0.6929	47	0.1935
Case-13	27	0.1460	52	1.5916	76	0.6783	92	0.8716
	111	0.8800	113	1.2111	51	0.3924	97	1.2141
	71	1.4553	74	1.9814	48	0.1516	52	0.7196
	74	1.1841	84	1.2716	56	0.2267	76	0.9103
	53	0.8764	97	0.1425	52	0.3262	85	0.3911

Table 12. Optimal positioning and sizing of SCs for scenario 4.

Cases	NSGA -2		PSO		GWO		GWO-PSO	
	SCs Location	SCs Size (MVAr)	SCs Location	SCs Size (MVAr)	SCs Location	SCs Size (MVAr)	SCs Location	SCs Size (MVAr)
Case-10	69	0.3683	5	0.6186	45	0.5395	16	0.8859
	35	0.7996	111	0.8791	81	0.7605	49	0.6926
	75	0.8182	68	0.4768	74	0.7618	28	0.6991
Case-11	7	0.3598	65	0.5128	61	0.5898	9	0.2953
	75	0.6733	100	0.4838	71	0.7295	41	0.4587
	77	1.0000	56	0.5476	66	0.1924	72	0.9477
Case-12	111	0.9884	73	0.2574	52	0.4971	47	0.4543
	4	0.8163	67	0.9924	111	1.0000	74	0.4977
	70	0.9816	6	0.9711	50	0.4938	58	0.2046
Case-13	75	0.6120	75	0.2094	34	0.2979	112	0.3724
	7	0.6329	23	0.9019	35	0.5958	74	0.6310
	78	0.5705	70	0.5205	31	0.2898	106	0.5835

Table 13. Scenario 4's optimal objective parameters.

Algorithms	Cases	DFC (USD M)	EUC (USD M/year)	CPDN (USD M/year)	DGC (USD M)	DVT (p.u.)
NSGA -2	10	3.5	0.06689	0.26418	11.159	0.0402
	11	3.45	0.08294	0.59928	2.3499	0.0625
	12	3.432	0.11420	0.55862	9.9048	0.0790
	13	3.432	0.072511	0.39972	5.5265	0.0492
PSO	10	3.9352	0.067315	0.51552	8.4839	0.0792
	11	3.9352	0.069653	0.63463	3.4765	0.0713
	12	3.89	0.098993	0.59747	2.5659	0.0873
	13	3.89	0.089961	0.51552	8.4839	0.0792
GWO	10	3.3	0.065888	0.34226	10.766	0.0669
	11	3.3	0.089744	0.59830	2.0220	0.0732
	12	3.425	0.088993	0.47761	2.5499	0.0767
	13	3.425	0.076576	0.52962	4.8601	0.0707
GWO-PSO	10	3.4715	0.065773	0.40880	9.5935	0.0810
	11	3.48	0.070837	0.51632	1.7488	0.0720
	12	3.2135	0.079180	0.42562	2.1300	0.0693
	13	3.2135	0.067005	0.31404	4.7970	0.0408

Table 14 compares the outcomes of four scenarios. Hybrid GWO-PSO outperforms other algorithms in terms of performance. In case 13, the DVT decreased by 68.99%, 18.8%, and 4.8% in comparison to case 3, case 6, and case 9. In case 13, the CPDN decreased by 53.21%, 22.41%, and 7.68% in comparison to case 3, case 6, and case 9. The DGC is reduced to 5.1% and 1.7% in case 13 in comparison to cases 6 and 9. Similarly, the DFC and EUC were reduced to 22.56% and 19.8% in case 13 compared to all cases. Simultaneous optimal FCE, DGs, and SCs in the coupled DST and road network give the best economical solution for the proposed method.

Table 14. Four scenarios' comparison results.

Scenarios	Cases	Algorithm	DFC (USD M)	EUC (USD M/year)	CPDN (USD M/year)	DGC (USD M)	DVT (p.u.)
4	13	NSGA-2	3.432	0.072511	0.39972	5.5265	0.0492
		PSO	3.89	0.089961	0.51552	8.4839	0.0792
		GWO	3.425	0.076576	0.52962	4.8601	0.0707
		GWO-PSO	3.2135	0.067005	0.31404	4.7970	0.0408
3	9	NSGA-2	4.42101	0.090780	0.37133	5.9512	0.0447
		PSO	4.3830	0.1036180	0.3974	6.8717	0.044275
		GWO	4.3520	0.0846530	0.381101	5.0512	0.05014
		GWO-PSO	4.15	0.083618	0.3402	4.8811	0.04287
2	6	NSGA-2	4.421	0.09078	0.4081	6.2795	0.0462
		PSO	4.383	0.103618	0.4042	7.1965	0.0457
		GWO	4.352	0.084653	0.4454	6.2583	0.0508
		GWO-PSO	4.15	0.083618	0.4051	5.0561	0.0503

5. Conclusions

This paper proposes a multi-objective hybrid GWO-PSO algorithm for the simultaneous optimal planning of fast charging stations, distributed generators, and shunt capacitors in an integrated electric transportation system. The problem was formulated to minimize the objectives, such as the cost of the active power loss of the distribution network, the development cost of the FCE, EV user energy consumption cost, voltage deviations, and cost of DGs on an 118 bus distribution system. Various case studies regarding the individual stage-wise placement and simultaneous placement of fast charging stations, distributed generators, and shunt capacitors using the proposed method were performed. They showed that the proposed method outperformed the stage-wise placement of various components in terms of the reduced active power loss cost and reduced EV user cost, and maintained a better voltage profile. The hybrid GWO-PSO method yields a better profit via simultaneous optimal allocation than the stage-wise placement for an equivalent investment on charging stations and DGs. The amalgam GWO-PSO algorithm proves to be robust and reliable when compared with conventional algorithms. The present work can be extended with vehicle-to-grid technology.

Author Contributions: Conceptualisation, A.K.M. and S.R.S.; methodology, A.K.M., P.S.B. and S.R.S.; software, A.K.M.; validation, A.K.M. and P.S.B.; review and editing, A.K.M., P.S.B. and S.R.S. All authors have read and agreed to the published version of the manuscript.

Funding: Woosong University's Academic Research Funding—2022.

Institutional Review Board Statement: Not applicable.

Informed Consent Statement: Not applicable.

Data Availability Statement: Not applicable.

Conflicts of Interest: The authors declare no conflict of interest.

Abbreviations

The following abbreviations are used in this manuscript:

EVs	Electrical Vehicles
FCEs	Electric Vehicle Fast charging stations
DST	Distribution System

DGs	Distributed Generators
SCs	Shunt Capacitors
CPDN	Active power loss of distribution network cost
DVTs	Voltage Deviations
DFC	Development Cost of FCE
EUC	Energy Consumption of EV user cost
DGC	Cost of DGs
GWO	Grey Wolf Optimiser
PSO	Particle Swarm Optimisation
NTEV	Total number of EVs
TLBO	Teaching-Learning-Based Optimisation
TPL	Total power loss of the distribution network including EV load
TGL	Gross power loss of the distribution network without EV load
TNL	Transportation network without EV load
$EV_{n,z}$	Total number of committed EVs in zone
zn	Number of zones in the assumed study area
C_{fixed}	The fixed cost of charging stations
C_{land}	Land rental cost yearly
C_{cond}	Development cost of chargers
n_y	Number of years in the study period
$NC(i)$	Number of connectors in charging stations in the i^{th}FCE period
PR_{EV}	Probability of the charging of EVs in hour (h) in a day
P_{cg}	Charging connector rated power
$L(zn, i)$	Trajectory length between zone zn and the i^{th} FCE
CSE	Specific energy consumption of EVs
EP_h	Electricity price in dollars
n_s	Number of seasons
N_{hr}	Total number of hours of all seasons in a year
d	Index of DG
$P_{dg,d}$	Active power generated by d^{th} unit
$Cost_{INV,d}$	Cost of investment of each d^{th} unit
C_{INV}	Cost of investment
C_{OPR}	Cost of operation
C_{MAT}	Cost of maintenance
TL_h	Number of hours in a year
n_{yr}	Total number of years for the planning of DGs
n_{dg}	Number of DGs
nb	Bus number of the distribution system
$V(j)$	Voltage of j^{th} bus
N_{FCE}	Number of FCEs
NP_{FCE}	Number of possible FCEs

References

1. Amin, A.; Tareen, W.U.K.; Usman, M.; Ali, H.; Bari, I.; Horan, B.; Mekhilef, S.; Asif, M.; Ahmed, S.; Mahmood, A. A review of optimal charging strategy for electric vehicles under dynamic pricing schemes in the distribution charging network. *Sustainability* **2020**, *12*, 10160.
2. Mirzapour, F.; Lakzaei, M.; Varamini, G.; Teimourian, M.; Ghadimi, N. A new prediction model of battery and wind-solar output in hybrid power system. *J. Ambient Intell. Humaniz. Comput.* **2019**, *10*, 77–87.
3. Zheng, Y.; Dong, Z.Y.; Xu, Y.; Meng, K.; Zhao, J.H.; Qiu, J. Electric vehicle battery charging/swap stations in distribution systems: Comparison study and optimal planning. *IEEE Trans. Power Syst.* **2013**, *29*, 221–229.
4. Sortomme, E.; Hindi, M.M.; MacPherson, S.J.; Venkata, S.S. Coordinated charging of plug-in hybrid electric vehicles to minimize distribution system losses. *IEEE Trans. Smart Grid* **2010**, *2*, 198–205.
5. Amini, M.H.; Moghaddam, M.P.; Karabasoglu, O. Simultaneous allocation of electric vehicles' parking lots and distributed renewable resources in smart power distribution networks. *ISustain. Cities Soc.* **2017**, *28*, 332–342.
6. Xu, D.; Pei, W.; Zhang, Q. Optimal Planning of Electric Vehicle Charging Stations Considering User Satisfaction and Charging Convenience. *Energies* **2022**, *15*, 5027. https://doi.org/10.3390/en15145027.
7. Kalakanti, A.K.; Rao, S. Charging Station Planning for Electric Vehicles. *Systems* **2022**, *10*, 6. https://doi.org/10.3390/systems10010006.

8. Amry, Y.; Elbouchikhi, E.; Le Gall, F.; Ghogho, M.; El Hani, S. Electric Vehicle Traction Drives and Charging Station Power Electronics: Current Status and Challenges. *Energies* **2022**, *15*, 6037. https://doi.org/10.3390/en15166037.
9. Ma, J.; Zhang, L. A Deploying Method for Predicting the Size and Optimizing the Location of an Electric Vehicle Charging Stations. *Information* **2018**, *9*, 170. https://doi.org/10.3390/info9070170.
10. Yenchamchalit, K.; Kongjeen, Y.; Prabpal, P.; Bhumkittipich, K. Optimal Placement of Distributed Photovoltaic Systems and Electric Vehicle Charging Stations Using Metaheuristic Optimization Techniques. *Symmetry* **2021**, *13*, 2378. https://doi.org/10.3390/sym13122378.
11. Hassler, J.; Dimitrova, Z.; Petit, M.; Dessante, P. Optimization and Coordination of Electric Vehicle Charging Process for Long-Distance Trips. *Energies* **2022**, *14*, 4054. https://doi.org/10.3390/en14134054.
12. Campaña, M.; Inga, E.; Cárdenas, J. Optimal Sizing of Electric Vehicle Charging Stations Considering Urban Traffic Flow for Smart Cities. *Energies* **2021**, *14*, 4933. https://doi.org/10.3390/en14164933.
13. Shareef, H.; Islam, M.M.; Mohamed, A. A review of the stage-of the-art charging technologies, placement methodologies, and impacts of electric vehicles. *Renew. Sustain. Energy Rev.* **2016**, *64*, 403–420.
14. Gao, Z.; Mao, D.; Wang, J. Distribution grid response monitor. *IET Gener. Transm. Distrib.* **2019**, *19*, 4374–4381.
15. Purvins, A.; Covrig, C.F.; Lempidis, G. Electric vehicle charging system model for accurate electricity system planning. *IET Gener. Transm. Distrib.* **2018**, *12*, 4053–4059.
16. Zhang, T.; Chen, X.; Yu, Z.; Zhu, X.; Shi, D. A Monte Carlo simulation approach to evaluate service capacities of EV charging and battery swapping stations. *IEEE Trans. Ind. Inform.* **2018**, *14*, 3914–3923.
17. Fotouhi, Z.; Hashemi, M.R.; Narimani, H.; Bayram, I.S. A general model for EV drivers' charging behavior. *IEEE Trans. Veh. Technol.* **2019**, *68*, 7368–7382.
18. Fahmy, S.; Gupta, R.; Paolone, M. Grid-aware distributed control of electric vehicle charging stations in active distribution grids. *Electr. Power Syst. Res.* **2020**, *189*, 106697.
19. Yufei, W.; Chenglong, W.; Hua, X. A novel capacity configuration method of flywheel energy storage system in electric vehicles fast charging station. *Electr. Power Syst. Res.* **2021**, *195*, 107185.
20. Abdalrahman, A.; Zhuang, W. PEV charging infrastructure siting based on spatial–temporal traffic flow distribution. *IEEE Trans. Smart Grid* **2019**, *10*, 6115–6125.
21. Xu, Y.; Çolak, S.; Kara, E.C.; Moura, S.J.; González, M.C. Planning for electric vehicle needs by coupling charging profiles with urban mobility. *Nat. Energy* **2018**, *3*, 484–493.
22. Bitencourt, L.; Abud, T.P.; Dias, B.H.; Borba, B.S.; Maciel, R.S.; Quirós-Tortós, J. Optimal location of EV charging stations in a neighborhood considering a multi-objective approach. *Electr. Power Syst. Res.* **2021**, *199*, 107391.
23. Dong, X.; Mu, Y.; Xu, X.; Jia, H.; Wu, J.; Yu, X.; Qi, Y. A charging pricing strategy of electric vehicle fast charging stations for the voltage control of electricity distribution networks. *Appl. Energy* **2018**, *225*, 857–868.
24. Wang, Y.; Shi, J.; Wang, R.; Liu, Z.; Wang, L. Siting and sizing of fast charging stations in highway network with budget constraint. *Appl. Energy* **2018**, *225*, 1255–1271.
25. Xiang, Y.; Liu, J.; Li, R.; Li, F.; Gu, C.; Tang, S. Economic planning of electric vehicle charging stations considering traffic constraints and load profile templates. *Appl. Energy* **2016**, *178*, 647–659.
26. Miljanic, Z.; Radulovic, V.; Lutovac, B. Efficient placement of electric vehicles charging stations using integer linear programming. *Adv. Electr. Comput. Eng.* **2018**, *18*, 11–16.
27. Sadeghi-Barzani, P.; Rajabi-Ghahnavieh, A.; Kazemi-Karegar, H. Optimal fast charging station placing and sizing. *Appl. Energy* **2014**, *18*, 289–299.
28. Mohanty, A.K.; Babu, P.S. Multi Objective Optimal Planning of Fast Charging station and Distributed Generators in a Distribution System. In Proceedings of the IEEE 2nd International Conference On Electrical Power and Energy Systems (ICEPES), Bhopal, India, 10–11 December 2021. https://doi.org/10.1109/ICEPES52894.2021.9699774.
29. Battapothula, G.; Yammani, C.; Maheswarapu, S. Multi-objective simultaneous optimal planning of electrical vehicle fast charging stations and DGs in distribution system. *J. Mod. Power Syst. Clean Energy* **2019**, *7*, 923–934.
30. Injeti, S.K.; Thunuguntla, V.K. Optimal integration of DGs into radial distribution network in the presence of plug-in electric vehicles to minimize daily active power losses and to improve the voltage profile of the system using bio-inspired optimization algorithms. *Prot. Control Mod. Power Syst.* **2020**, *5*, 1–15.
31. Kumar, A.; Meena, N.K.; Singh, A.R.; Deng, Y.; He, X.; Bansal, R.C.; Kumar, P. Strategic integration of battery energy storage systems with the provision of distributed ancillary services in active distribution systems. *Appl. Energy* **2019**, *253*, 113503.
32. Chang, S.; Niu, Y.; Jia, T. Coordinate scheduling of electric vehicles in charging stations supported by microgrids. *Electr. Power Syst. Res.* **2019**, *199*, 107418.
33. Ghofrani, M.; Majidi, M. A comprehensive optimization framework for EV-Renewable DG coordination. *Electr. Power Syst. Res.* **2021**, *194*, 107086.
34. Ahmad, F.; Alam, M.S.; Shariff, S.M.; Krishnamurthy, M. A cost-efficient approach to EV charging station integrated community microgrid: A case study of Indian power market. *IEEE Trans. Transp. Electrif.* **2021**, *5*, 200–214.
35. Rahmani-Andebili, M.; Shen, H.; Fotuhi-Firuzabad, M. Planning and operation of parking lots considering system, traffic, and drivers behavioral model. *IEEE Trans. Syst. Man, Cybern. Syst.* **2018**, *5*, 1879–1892.

36. Rajesh, P.; Shajin, F.H. Optimal allocation of EV charging spots and capacitors in distribution network improving voltage and power loss by Quantum-Behaved and Gaussian Mutational Dragonfly Algorithm (QGDA). *Electr. Power Syst. Res.* **2021**, *194*, 107049.
37. Biswas, P.P.; Mallipeddi, R.; Suganthan, P.N.; Amaratunga, G.A. A multiobjective approach for optimal placement and sizing of distributed generators and capacitors in distribution network. *Appl. Soft Comput.* **2017**, *60*, 268–280.
38. Bilal, M.; Rizwan, M. Integration of electric vehicle charging stations and capacitors in distribution systems with vehicle-to-grid facility. *Energy Sources, Part A: Recovery, Utilization, and Environmental Effects* **2021**, 1–30. https://doi.org/10.1080/15567036.2021.1923870
39. Kennedy, J.; Eberhart, R. Particle swarm optimization. In Proceedings of the ICNN'95—International Conference on Neural Networks, Perth, WA, Australia, 27 November–1 December 1995; Volume 4, pp. 1942–1948. https://doi.org/10.1109/ICNN.1995.488968.
40. Mirjalili, S.; Mirjalili, S.M.; Lewis, A. Grey wolf optimizer. *Adv. Eng. Softw.* **2014**, *69*, 46–61.
41. Mohanty, A.K.; Babu, P.S. Optimal placement of electric vehicle charging stations using JAYA algorithm. In *Recent Advances in Power Systems*; Springer: Singapore, 2021; pp. 259–266.
42. Deb, K.; Pratap, A.; Agarwal, S.; Meyarivan, T.A.M.T. A fast and elitist multiobjective genetic algorithm: NSGA-II. *IEEE Trans. Evol. Comput.* **2002**, *42*, 182–197.
43. Shukla, A.; Verma, K.; Kumar, R. Multi-Objective Synergistic Planning of EV Fast Charging Stations in Distribution System Coupled with Transportation Network. *IET Gener. Transm. Distrib.* **2019**, *15*, 3421–3432.
44. Singh, N.; Singh, S.B. Hybrid algorithm of particle swarm optimization and grey wolf optimizer for improving convergence performance. *Journal of Applied Mathematics* **2017**, *2017*, 2030489.
45. Di Fazio, A.R.; Russo, M.; De Santis, M. Zoning evaluation for voltage control in smart distribution networks. In Proceedings of the 2018 IEEE International Conference on Environment and Electrical Engineering and 2018 IEEE Industrial and Commercial Power Systems Europe (EEEIC/I & CPS Europe), Palermo, Italy, 12–15 June 2018; pp. 1–6.
46. Jia, Z.; Qi, F. Network Clustering Algorithm Based on Fast Detection of Central Node. *Sci. Program.* **2022**, *2022*, 1058–9244. https://doi.org/10.1155/2022/4905190.
47. Mirjalili, S.; Saremi, S.; Mirjalili, S.M.; Coelho, L.D. Multi-objective grey wolf optimizer: A novel algorithm for multi-criterion optimization. *Expert Syst. Appl.* **2016**, *47*, 106–119.